Environmental Earth Sciences (2018) 77:644
https://doi.org/10.1007/s12665-018-7747-1

ORIGINAL ARTICLE

A survey of groundwater quality in Tulum region, Yucatan Peninsula, Mexico

Renaud Saint-Loup[1] · Théo Felix[1] · Axaycatl Maqueda[1] · Arnulf Schiller[2] · Philippe Renard[1]

Received: 21 December 2017 / Accepted: 6 August 2018 / Published online: 15 September 2018

Abstract

The city of Tulum, in the state of Quintana Roo (Mexico) depends almost exclusively on groundwater for water supply. The groundwater is exploited from a coastal aquifer which contains a karst network that is considered as one of the largest ones on earth. Given the nature of karst aquifers, the whole area is very sensitive to contaminants and bacteria transport, because flow paths, residence time and degradation rates differ significantly from what can be observed in the porous aquifer. The present study focuses on isotopes (^{18}O and ^{2}H), dissolved ions' concentration and *Escherichia coli* (*E. coli*). The result of our survey points out the anthropic impact on groundwater quality. Furthermore, the chloride concentrations illustrate the influence of seawater mixing and geological heterogeneity over the study area. Due to an exponential growth of the tourism industry, the needs in terms of water supply and water treatment increase significantly. Tulum is a coastal city, facing a coral reef and is bordered by the Sian Ka'an biosphere reserve, therefore, an environmental issue is added to the sanitary issue, both being the basis of the local economic development. Our results show that *E. coli* remains a major issue, as several samples tested were contaminated, in particular those in the city center. Ions' survey shows an anthropic impact through nitrate, phosphate and fluoride concentrations, but the obtained values are not alarming. Considering the saline intrusion, chloride concentrations indicate that the area below the Tulum city center seems to be less permeable (and maybe less karstified) than the surrounding areas, as groundwater is less subject to seawater mixing than other sampling sites at similar distance to the coast.

Keywords Karst · Mexico · Groundwater quality · Contamination · Seawater intrusion

Introduction

The state of Quintana Roo constitutes the eastern part of the Yucatan Peninsula (Online Resource 1). Located on Mexico's Caribbean coast, the city of Tulum which had about 28,000 inhabitants in 2010 (Instituto Nacional de Estadistica y geografia) is facing the Mesoamerican reef which is the second largest reef in the world, but it had more than 50% loss of coral cover over the last 20 years, possibly linked with eutrophication (Metcalfe et al. 2011). A few kilometers south of Tulum, the Sian Ka'an biosphere reserve extends over 5280 km^2 and supports wetlands, coral reefs and tropical forests. In addition to being a shelter for biodiversity and indigenous species, the wetlands provide a protection from impacts of hurricanes (Gondwe et al. 2010a, b). The wetlands of the Sian Ka'an biosphere reserve, listed as an UNESCO World Heritage site, represent an additional value for local tourism. The area first developed tourism with an excursion from the northward hotels to the Mayan ruins. The State of Mexico has decided to develop infrastructures and accommodation capacities with concrete roads in the city of Tulum and has also planned a project of building an airport. This policy has led to a population growth rate over 14% per year in some areas (Hernández-Terrones et al. 2011) and Tulum is the fastest growing town in Mexico. Tourism represents 90.2% of the gross state income (Hausman 2009) and the number of hotel rooms has increased by 30% from 2010 to 2016 (Secretaria de Turismo de Mexico).

Electronic supplementary material The online version of this article (https://doi.org/10.1007/s12665-018-7747-1) contains supplementary material, which is available to authorized users.

✉ Renaud Saint-Loup
renaudsaintloup@hotmail.com

[1] Centre for Hydrogeology and Geothermics, Université de Neuchâtel, 11 Rue Emile Argand, 2000 Neuchâtel, Switzerland

[2] Geological Survey of Austria, Neulinggasse 38, 1030 Vienna, Austria

The only source of freshwater in eastern Quintana Roo is a lens of groundwater whose thickness ranges from a few meters up to 100 m overlaying saline water (Gondwe et al. 2010). This groundwater provides water to wetlands, forests and human amenities through a karstic network. Due to its karstic environment, the unconfined aquifer of the state of Quintana Roo is particularly sensitive to anthropic pollution due, among others, to sewages as it is a common practice to inject them under the freshwater lens (Leal-Bautista et al. 2013). The touristic development of the city of Tulum leads to dramatic issues in terms of public health; in a year, a raise of 30% in gastrointestinal diseases has been reported by Tulum's Red Cross director (Lopez 2016). Furthermore as a coastal area, this aquifer is subject to saline intrusion which produces a variable salinity in the pumped water depending on the location of wells.

The average use of groundwater in the Yucatan Peninsula is 61% for agriculture, 20% domestic and 19% industrial (CONAGUA). Consumption is 1.63 m^3 day/per capita (Bauer-Gottwein et al. 2011), abstraction about 1.4% of precipitation, and concerning water, the area is facing more a quality problem than a scarcity issue. As the eastern part of the Peninsula is much more touristic, the percentage of water assigned to agriculture is lower in eastern Quintana Roo than in the rest of Yucatan Peninsula (YP).

A common practice is the injection of untreated or poorly treated sewage under the freshwater lens (Leal-Bautista et al. 2013). Considering the city of Tulum, the connection to the municipal wastewater network varies, and it is obvious that some houses are not connected and the maintenance of wastewater treatment systems like septic tanks remains a major problem. Leal-Bautista et al. (2013) did a sampling campaign from 2008 to 2012 in the vicinity of Tulum. The study indicates that groundwater is contaminated by *Escherichia coli* and that the rapid rise in population increases the risk of contamination of drinking water supply.

The objectives of this study are to evaluate the quality of the groundwater in the karstic aquifers surrounding the city of Tulum. It is important to evaluate the degree of contamination of the aquifer, the possible impact of the city on the groundwater, but also the fluxes of nutrients or contamination toward the coral reef and the Sian Ka'an reserve. In particular, our survey will focus on two types of contamination: bacteriological contamination with measurements of *E. coli*, and solute contamination with the determination of major ion concentrations (fluoride, nitrite, chloride, bromide, nitrate, phosphate, sulfate, lithium, sodium, ammonium, potassium, magnesium, calcium, strontium and total alkalinity). These data will allow mapping of the water quality. The contribution of seawater will also be investigated specifically.

The document is structured as follows. "Hydrogeological setting" section describes the hydrogeological setting of the study area focusing on hydrology, geology and lithology, groundwater flow and saline intrusion. "Material and methods" section describes the details about the sampling sites and analytic methods; "Results and discussion" displays the results and discussion.

Hydrogeological setting

Hydrology

Local climate is tropical with a wet season from May to September and a dry season from October to April. Precipitation occurs in Yucatan Peninsula (YP) with an east to west gradient (1500 mm $year^{-1}$ on Caribbean coast and a minimum of 550 mm $year^{-1}$ inland), 80% during the wet season (Smart et al. 2006). Average annual evapotranspiration between 2004 and 2008 varied spatially from 350 to 2500 mm $year^{-1}$; a higher value corresponds to the coastal area, where evapotranspiration rate exceeds the recharge rate. The average recharge rate in the Yucatan Peninsula is 150 mm $year^{-1}$ (Bauer-Gottwein et al. 2011).

Geology and lithology

The Yucatan Peninsula is a 300,000 km^2 carbonate platform in which the land spans about 165,000 km^2. It is made of limestone, dolomites and evaporites with over 1500 m thickness (Bauer-Gottwein et al. 2011). The two main structural features found in the vicinity of the field area are the Rio Hondo fault system and the Holbox fracture zone trending, respectively, SW–NE and SSW–NNE. Rio Hondo is a normal fault located in the southern part of Quintana Roo and extends to Belize, and the Holbox fracture zone, a possibility due to the Eocene Caribbean plate movement, is visible as flat-bottomed elongated solution depressions (sabanas). It runs NNE–SSW, from 10 km inland of Tulum to Isla Holbox on the north coast of the Peninsula.

The outcrops are gradually younger in the direction of the shelf margin going from upper Cretaceous to Holocene (Bauer-Gottwein et al. 2011). On the eastern margin, the top of the platform is a 12 m thick Pleistocene carbonate deposited during the last highstand of sea level (Ward 2003). At the end of the Cretaceous period, an asteroid hit the north of the Yucatan Peninsula producing a 200 km large impact crater known as Chicxulub. Impact breccias related to the Chicxulub impact have been logged at 160 m depth in the north-eastern part of the Peninsula (Ward et al. 1995), ejecta linked to the impact outcrops in southern Quintana Roo (Bauer-Gottwein et al. 2011), and evaporites are found from 1500 to 2000 m depth and become much shallower when going northward (Smart et al. 2006). The Tertiary limestone of the Yucatan Peninsula that corresponds to the upper part

of the aquifer are deposited sub-horizontally (Smart et al. 2006) which indicates little deformation during the Tertiary period.

Eastern Quintana Roo is mapped as lower, middle and upper Pleistocene limestones, units that consist of platform margin corals and back reef corals. They are separated by caliche crusts corresponding to the subaerial diagenesis during low stands, and due to their low conductivity, these caliche crusts possibly acts as aquitards. The upper Pleistocene unit corresponds to lagoon limestone, a low energy environment producing skeletal wackestone and mudstone up to 2.6 m thick. Skeletal constituents are mollusks, foraminifer and bivalves that are composed of aragonite and calcite (Ward 2003).

Dolomites occur in the phreatic zone in the meters below the water table; the composition varies from $Ca_{57}Mg_{43}$ to $Ca_{62}Mg_{38}$ (Ward 2003).

Groundwater flow

The aquifer of Quintana Roo is a coastal aquifer, a fresh groundwater lens that overlays a warmer saline intrusion. The interface between both is called as the mixing zone which contains brackish water (MZ). There are almost no lakes or rivers in the YP. Soils in the area of Tulum are very thin (few centimeters) and epikarst with high porosity and conductivity outcrops frequently. Meteoric water then quickly infiltrates small fractures, with almost no filtration from soils, and the karst then becomes particularly sensitive to pollution (Gondwe et al. 2010).

After a quick infiltration through a thin layer of soil, epikarst and fractures, freshwater in the area of Tulum flows through an anastomosing cave network going up to 12 km inland (Smart et al. 2006). Two main karstic systems that appear to be some of the largest worldwide are in the vicinity of Tulum, Sac Aktun and Ox Bel'Ha which are, respectively, 257 and 270 km long, with Naranjal being in the northern part of Ox Bel'Ha (QRSS 2016). Depth of the conduits in the study area varies from the water table up to 30 m deep, but the general trend for mean conduit depth is to increase when it reaches inland (Smart et al. 2006).

These networks made up of fractures and conduits represent 99.8% of flow, whereas storage occurs in matrix at 97.1% (Leal-Bautista et al. 2013). Discharge occurs either at the coast, often as caletas and bays, or within the Mesoamerican coral reef. Coastal outflow rate is estimated at 0.3–0.4 $m^3\ km^{-1}\ s^{-1}$ (Bauer-Gottwein et al. 2011).

Porosity in the aquifer is considered to be triple, the matrix porosity has a three-dimensional flow, bedding plane and faults have a two-dimensional flow and conduits have a one-dimensional flow (Beddows 2004). Two types of conduit are present in Quintana Roo, first is the fissure passages that are 5–10 m high, 0.5–2 m wide and tens of meters long, second is the elliptical tubular passages that are 1.1–5 times wider than higher (from 2 to 30 m wide), the widest part corresponding to the modern mixing zone (Smart et al. 2006).

Worthington provides the following value for the Quintana Roo aquifer (Worthington et al. 2000).

- Porosity: matrix 17%, fracture 0.1%, channel 0.5%
- Proportion of storage: matrix 96.6%, fracture 0.6%, channel 2.8%
- Hydraulic conductivity ($m\ s^{-1}$): matrix 7×10^{-5}, fracture 1×10^{-3}, channel 4×10^{-1}

Groundwater velocity were measured in fractures from mm/s range (Schiller A., pers. com) to 12 $cm\ s^{-1}$ whereas, in the matrix, values were in the range of 10^{-2} $cm\ s^{-1}$ (Vuilleumier et al. 2013). Average hydraulic gradient in the field area is 6.10^{-5} (Smart et al. 2006).

The Quintana Roo karstic aquifer is an intermediate between telogenetic karst in which the organized conduit network is developed and eogenetic karsts, corresponding to a relatively short time between burial and exposure. The second type is diagenetically immature with high matrix porosity and presence of metastable carbonates like aragonite (Smart et al. 2006).

Groundwater, in the coastal area flows perpendicular to the coastline (Fig. 1), nevertheless, due to its particular porosity and permeability, the Holbox fracture zone represents a preferential flow path.

Electromagnetic studies have been performed over the area of Tulum and indicate a higher subsurface electrical conductivity in the fracture zone corresponding to a higher porosity and permeability. Porosity in Holbox zone is 0.41 ± 0.13, whereas outside the zone, porosity is 0.25 ± 0.1 (Gondwe et al. 2012). Flow path follows the lineament of the fracture zone with a northward direction. Cenotes and lagoons, as surface manifestations of a zone of high permeability in the subsurface, follow the lineament of the Holbox fracture zone. Conduits and thus links between the Holbox fracture and the fieldwork area are not proved at the moment.

Saline intrusion

As a coastal aquifer, the YP freshwater lens (FWL) is subject to saline intrusion. Because of a high hydraulic conductivity, the water table in YP is low. Thickness of FWL in the coastal karstic plain of Tulum is influenced by sea tide and the presence of conduits. At the YP scale, it seems that the Ghyben–Herzberg model is respected (Bauer-Gottwein et al. 2011) but, due to conduits, it does not correspond to a smooth increase in depth. An electromagnetic airborne survey has been operated by the Geological Survey of Austria (GSA) in the coastal karst plain of Tulum, and two transects of subterranean electrical conductivity illustrate the

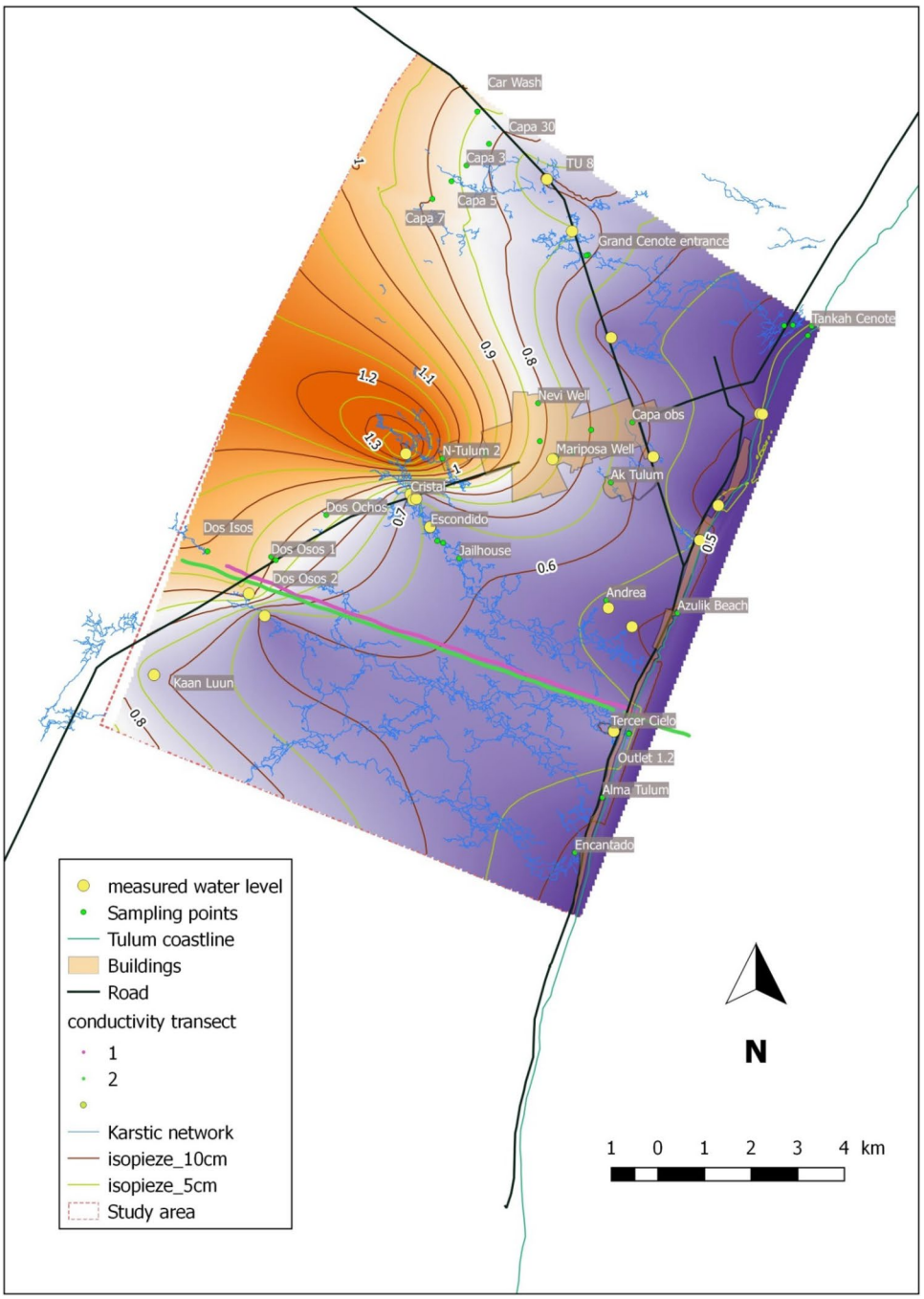

Fig. 1 Map of the study area, showing in background the interpolated groundwater level over the study area, the yellow dots correspond to sites where measurements were made, red color corresponds to higher water level (up to 1.45 m), purple color represent the lower water level (0.47 m). This map is only indicative since the piezometry is known to be highly influenced by the presence of the karstic conduit (in blue in the map) but because of insufficient data this dependence is not illustrated on the map. Overall, the map shows groundwater flow from the inland side of the site on the western part to the coast on the eastern side of the site

interpreted position of the halocline in the vicinity of Tulum Fig. 2.

Saline intrusion can occur up to 100 km inland. The interface between FWL and seawater is the mixing zone which contains brackish water (Null et al. 2014).

Within this mixing zone, different flows occur, a coastward freshwater outflow leads a saline water outflow and an inflow of saline water at depth compensates the saline coastward outflow. A vertical flow due to density-driven buoyancy occurs in the karst of Florida in case of wastewater injection (Dillon et al. 2000), and as injection of wastewater in the karst is a common practice in Tulum, a vertical flow is also possible. Furthermore, in case of fresh water input (meteoric water infiltration), GWL rise might change the halocline level and thus trigger vertical flow.

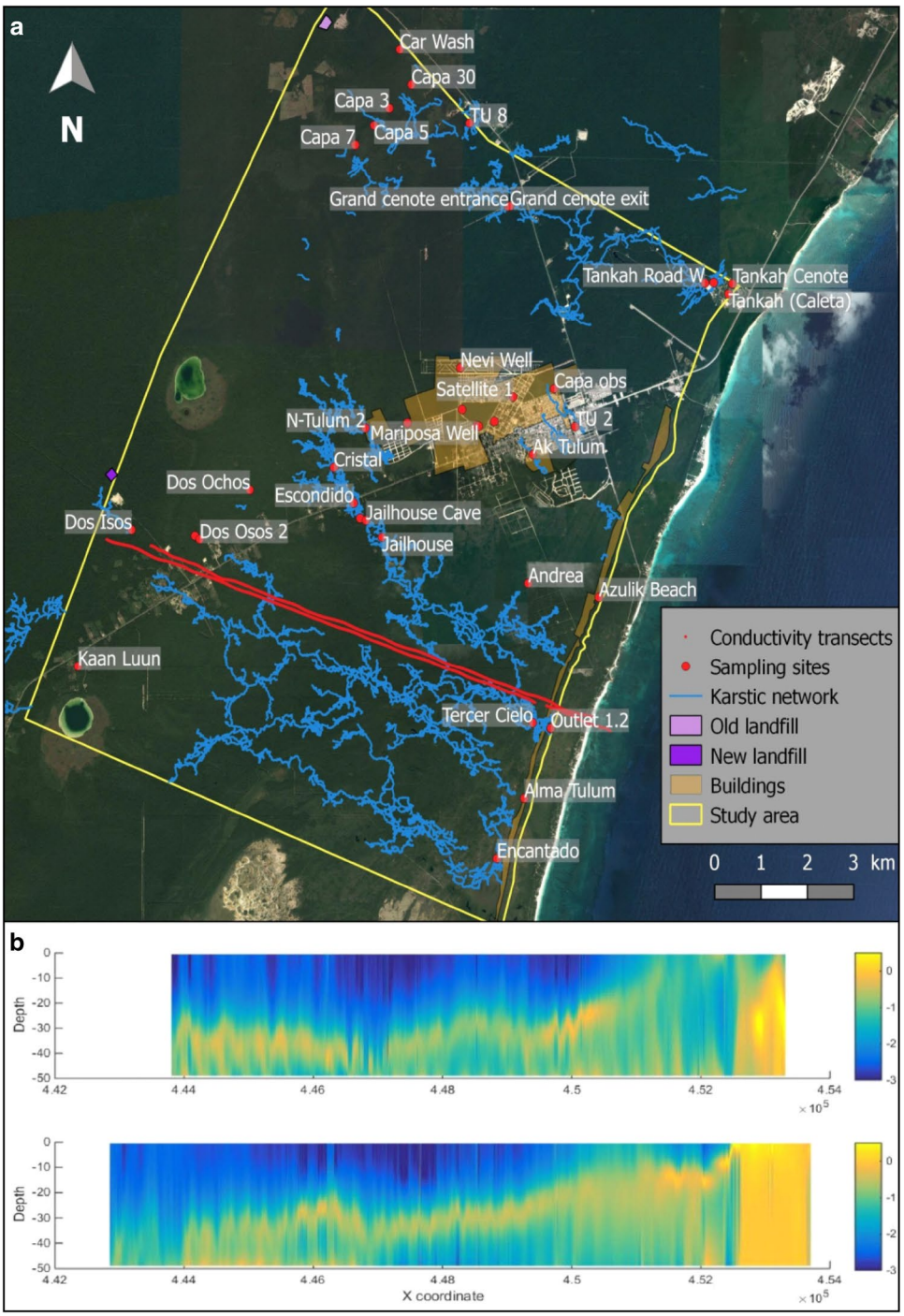

Fig. 2 Map of the study area (**a**) and electric conductivity profiles (**b**). On **a**, red dots represent sampling sites and blue lines represent the part of the karstic network that is known and mapped by the cave divers. The red lines made of small red dots represent two electric conductivity profiles made by the GSA in the vicinity of Tulum, each line is about 10 km long. On **b**, the blue color represents fresh water lens (conductivity is also influenced by porosity which we do not know), the yellow color represents the saline water body, and green color represents a lower conductivity probably due to the matrix. Depth of investigation is 50 m and electrical conductivity is in log10 (S/m) (Schiller A., pers com)

Materials and Methods

Sampling sites

The sampling sites are located in and around the city of Tulum (Fig. 2), i.e., the study area which has a rectangular shape and is lined up on the coast of Yucatan. The study area covers roughly 150 km^2, 11 km wide oriented NW–SE and 14 km long oriented SW–NE, and the Holbox fracture zone represents the inland boundary of the area. GPS coordinates and the time of sampling are provided in Table 1.

Method

In the field, values of dissolved oxygen, pH and conductivity were measured with HACH HQ 40d multi and samples were filtrated, using a 0.45 µm syringe filter. Thirty-nine samples

Table 1 List of sampling sites' coordinates (in degrees, projection WGS84) and sampling time

ID	Latitude	Longitude	Date	Time	Type of site
Encantado	20.1315	− 87.46644	25.03.2017	15h25	cenote
Tercer Cielo	20.15542	− 87.45905	25.03.2017	16h55	cenote
Dos Isos	20.18949	− 87.54181	26.03.2017	16h15	cenote
Dos Osos 1	20.18843	− 87.52876	26.03.2017	17h20	cenote
Dos Ochos	20.19651	− 87.51743	26.03.2017	18h30	cenote
Cristal	20.20047	− 87.50007	28.03.2017	12h30	cenote
Escondido	20.1942	− 87.49598	28.03.2017	13h45	cenote
Juan Cenote	20.1915	− 87.49467	28.03.2017	14h45	cenote
Car Wash	20.27418	− 87.48644	28.03.2017	15h45	cenote
Tankah Cenote	20.23286	− 87.41784	29.03.2017	13h45	cenote
Tankah Road	20.23306	− 87.42172	29.03.2017	15h00	cenote
Gran Cenote Entrance	20.24648	− 87.46408	30.03.2017	12h00	cenote
Gran Cenote Exit	20.24657	− 87.46372	30.03.2017	12h30	cenote
Jailhouse	20.18816	− 87.49015	30.03.2017	14h30	cenote
Ak Tulum	20.20277	− 87.45903	05.04.2017	12h30	cenote
N-Tulum 2	20.2074	− 87.49359	07.04.2017	13h20	cenote
Tankah Road W	20.23296	− 87.42351	07.04.2017	14h10	cenote
Jailhouse Cave	20.19113	− 87.49347	08.04.2017	12h45	conduit
Kaan Luun	20.16542	− 87.55288	26.03.2017	15h25	cenote
Outlet 1.1	20.15442	− 87.45537	25.03.2017	17h50	outlet
Outlet 1.2	20.15449	− 87.45532	25.03.2017	18h25	outlet
Tankah (Caleta)	20.23106	− 87.41864	29.03.2017	13h10	outlet
TU 8	20.26118	− 87.47204	04.04.2017	16h20	piezometer
Capa obs	20.21436	− 87.45463	10.04.2017	12h00	piezometer
Capa 30	20.26798	− 87.48406	10.04.2017	13h50	piezometer
Dos Osos 2	20.18781	− 87.52777	26.03.2017	17h45	private well
Temple Well	20.20858	− 87.46696	04.04.2017	17h30	private well
Well Front Mariposa	20.20784	− 87.47058	04.04.2017	18h05	private well
Mariposa Well	20.20773	− 87.47023	04.04.2017	18h30	private well
Satellite 1	20.21289	− 87.46309	05.04.2017	11h30	private well
Alma Tulum	20.14211	− 87.46078	05.04.2017	16h10	private well
Mayan Pax	20.21071	− 87.47362	05.04.2017	17h10	private well
N-Tulum 1	20.2083	− 87.48491	07.04.2017	13h00	private well
Andrea	20.18007	− 87.45998	09.04.2017	21h00	private well
Nevi Well	20.21804	− 87.47398	10.04.2017	16h00	private well
Capa 7	20.25738	− 87.49568	10.04.2017	12h50	public well
Capa 5	20.26079	− 87.49176	10.04.2017	13h15	public well
Capa 3	20.26382	− 87.48867	10.04.2017	13h30	public well
Azulik Beach	20.17758	− 87.44539	28.03.2017	16h55	Sea

The sites are clustered in four groups: cenote or conduit, outlet (freshwater springs), piezometer or well and sea

were taken for analysis of anions, cations and *E. coli* and 12 for total alkalinity.

Phosphate and nitrate concentrations were analyzed within the 12 h following sampling with HATCH DR1900. Reactives used were USEPA PhosVer 3 for phosphate and SulfaVer 4 for sulfate.

Major ions were analyzed at the University of Neuchâtel (CHYN) using a DIONEX ICS-1600 Ion Chromatography System (Thermo Fisher Scientific Inc.). Due to the high salinity of samples, dilution was applied for each sample (the dilution factors are provided in the Electronic supplement material 16). Twelve samples for total alkalinity data were collected in 250 ml plastic bottles in Encantado, Tercer Cielo, Kaan Luun, Dos Isos, entrance and exit of Gran Cenote, Temple Well, Alma Tulum, Tankah Road West, Capa Obs, Capa 7 and Capa 30. Analyses were made at CHYN with TITRINO 848. The ionic balance (IB) was computed for these 12 samples using Eq. (1).

$$\mathrm{IB}(\%) = \frac{\sum \mathrm{Cations} - \sum \mathrm{Anions}}{\sum \mathrm{Cations} + \sum \mathrm{Anions}} \times 100 \quad (1)$$

The results of IB vary from − 3% to − 0.2%, indicating that the ionic analysis for these samples are acceptable (− 5%

< range < 5%). $HCO3^-$ concentrations for the other samples were deduced from the assumption of a perfect ionic balance (Table 2).

The calculated total alkalinity has not been taken into account for the site N Tulum 2 because the calculated value was close to 0 mg/l of $HCO3^-$ which is highly improbable in karstic environment. An extra analysis of total alkalinity was made at CHYN and gave a value of 398.35 mg/l of $HCO3^-$.

Ionic strength (I) has been calculated using Eq. (2):

$$I = \frac{1}{2} \sum [i].Z_i^2 \quad (2)$$

With:

- $[i]$ the concentration of species I
- Z_i the charge of the ion

The saturation indices (SI) of fluorite, calcite, dolomite, hydroxyapatite and aragonite have been calculated with PHREEQC, using the Davis equation valid up to an ionic strength of about 0.5 (the maximum ionic strength is 0.65 in Azulik beach).

$\Delta^{18}O$ and $\Delta^{2}H$ were measured at CHYN using PICARRO L2130-I. For bacteria analysis, samples were collected in 250 ml plastic bottles sterilized by a 15 mn immersion in boiling water. Analyses were made within 12 h following sampling. A membrane filtration of 100 ml of water was made with S-PAK membrane filter and was deposited in a *Petri box R-Biopharm Compact Dry EC*, both being stored in an incubator for 24 h. Colony-forming units (CFU) were counted manually at the end of incubation time. A campaign of sampling has been conducted in March 2016 by Gregory Kaeser. Data were analyzed and plotted using Aquachem 5.1 software. To improve the clarity of plots, legends were simplified to four groups:

- Sea: represents the sample taken in Azulik beach and corresponds to sea water end member
- Outlet: represents the exit flow of karstic network in the sea
- Cenote: represents samples made in cenotes, conduits, and lagoon.
- Well: represents samples made in wells and piezometers

Contamination maps were created with QGIS 2.18 program.

The groundwater level map over the study area (Fig. 1) was obtained using kriging with a locally varying mean (LVM). The LVM is estimated using a linear regression of the groundwater levels (y) versus distance (x) to the coast:

$$y = 5.10^{-5} \times x + 0.47 \quad (3)$$

Results and discussion

All the results of the water quality analysis are provided in the form of extensive tables and maps in the Electronic supplement materials. In the following sections, we summarize the main findings and illustrate them with summary figures and maps.

Escherichia coli

Escherichia coli values are ranked in 4 categories: 0 CFU/100 ml, 1–50 CFU/100 ml, 51–300 CFU/100 ml, more than 300 CFU/100ml: too numerous to count (TNTC). The aim of this ranking is to provide an easy reading grid as considering analysis conditions (numerous electricity cut-off during incubation); our goal is to provide qualitative more than quantitative results.

In 2017, concentrations are variable within the city area with a range of values between 0 CFU/100 ml in Nevi well and a mat of *E. coli* bacteria considered as TNTC in Well Front Mariposa.

Comparison between 2016 and 2017 results shows a great variability, but the general trend is a lower concentration of CFU/100 ml in 2017 (Fig. 3).

Nevertheless, *E. coli* is also found in touristic places like cenotes and outlets. Tankah Cenote is a touristic cenote located at about 200 m from the sea, 15 CFU/100 ml were obtained with the sampling, whereas sampling made in caleta Tankah, Tankah road and Tankah road west shows no contamination in 2017.

Gran Cenote is a very touristic place, with an average attendance of 400 people per day in March (personal discussion with staff). Two samples were taken at about 50 m from one to another, one upstream where the water arrives in the cenote from a subterranean conduit and the other downstream where the water leaves the cenote through subterranean conduits. No contamination was found upstream, whereas downstream, a mat of *E. coli* was found which was too numerous to count (TNTC).

AK Tulum is a cenote located in a newly developed area made of high standing condos. The cenote was previously used by locals for laundry cleaning and was partly filled with various wastes. Rehabilitation has been operated since 2016 and the cenote now looks clean. *E. coli* results show no contamination, whereas the same cenote sampled in 2016 had a concentration over 300 CFU/100 ml (Electronic supplement material 10).

Our results show that presence of *E. coli* is correlated with human activities. Concentrations are generally higher in urban areas like Tulum city center which could be a result of leakage from septic tanks. Figure 3 show a

Table 2 Summary table of anions and cations' concentrations (mg/l) for each sampling site

ID	Fluoride	Chloride	Bromide	Nitrate	Phosphate	Sulfate	HCO3	Sodium	Ammonium	Potassium	Magnesium	Calcium
Capa 30	0.00	106.35	0.29	0.59	0.06	15.14	251.32	55.15	0.14	6.42	6.94	82.45
Well Front Mariposa	0.31	110.94	0.38	12.11	0.23	37.96	232.63	64.18	0.00	8.82	10.04	82.45
TU 8	0.14	105.09	0.46	1.34	0.81	17.34	356.63	62.90	8.62	4.54	11.27	99.79
Mayan Pax	0.19	260.10	0.75	7.56	0.20	52.48	309.41	146.24	2.32	10.20	18.03	108.53
Temple Well	0.32	251.32	0.75	28.48	0.11	58.95	357.95	158.88	0.00	12.45	23.89	96.17
Nevi Well	0.00	279.01	0.82	25.42	0.53	52.67	368.27	150.26	3.96	8.87	15.10	137.98
Mariposa Well	0.44	329.99	0.96	7.49	0.69	59.03	251.33	181.75	2.90	11.15	23.84	90.70
Capa obs	0.00	334.99	0.93	12.74	0.08	51.08	357.70	184.36	4.92	8.83	22.74	105.25
N Tulum 1	0.00	334.07	1.15	25.49	0.06	60.19	317.62	177.63	6.19	11.29	25.64	117.08
Kaan Luun	0.00	573.79	1.91	1.19	0.07	90.02	231.80	299.29	1.09	10.06	51.43	71.59
Dos Isos	0.00	503.50	1.57	9.45	0.08	77.73	433.59	263.64	2.00	8.26	49.45	135.63
N Tulum 2	0.00	561.76	1.78	8.05	0.07	67.04	398.35	223.60	1.54	8.58	33.16	87.04
Capa 5	0.00	531.14	1.75	7.93	0.08	78.88	474.91	285.83	2.37	8.43	53.97	147.11
Capa 3	0.00	538.25	1.79	8.41	0.08	80.82	414.63	282.55	0.00	7.89	52.56	140.40
Satellite 1	0.30	547.57	1.51	8.66	1.54	94.45	420.60	300.41	5.08	13.20	47.24	139.59
Dos Osos 1	0.00	633.76	2.06	8.18	0.05	95.56	383.68	332.11	0.00	10.11	56.59	139.34
Capa 7	0.00	620.89	2.06	7.62	0.08	90.64	435.05	325.78	2.37	9.48	56.19	148.26
Car Wash	0.00	649.13	1.99	8.49	0.02	98.34	415.14	345.50	0.00	10.64	59.78	142.38
Dos Osos 2	0.00	723.36	2.30	8.96	0.10	109.75	361.69	372.00	2.54	11.80	61.99	141.68
Dos Ochos	0.00	782.43	2.43	9.20	0.05	117.71	387.11	413.97	0.00	12.75	66.93	144.40
Grand Cenote exit	0.00	881.45	2.79	9.22	0.07	135.91	457.74	467.52	0.00	14.20	73.94	153.76
Grand Cenote entrance	0.00	889.03	2.73	9.26	0.07	136.82	455.79	468.31	0.00	14.50	73.52	152.96
Cristal	0.00	962.30	3.05	7.84	0.07	148.16	390.51	517.84	0.00	16.53	78.97	147.30
Juan Cenote	0.00	1035.69	3.26	8.08	0.01	156.33	407.14	562.40	0.00	18.23	84.55	148.82
Jailhouse	0.00	1096.12	3.51	5.15	0.04	166.20	377.63	588.51	0.00	19.29	86.82	149.48
Tankah Road West	0.00	1219.00	4.03	0.31	0.12	193.24	424.56	674.85	0.00	24.99	91.84	150.68
Escondido	0.00	1284.01	4.20	8.12	0.01	197.40	471.26	718.51	0.00	23.73	103.74	157.09
Jailhouse Cave	0.00	1450.81	4.99	6.83	0.04	224.09	393.83	784.05	5.51	28.99	112.54	156.41
Ak Tulum	0.00	1789.40	5.67	8.15	0.11	266.66	324.32	956.92	0.00	31.26	129.75	169.26
Alma Tulum	0.57	1867.93	5.97	22.80	0.16	217.16	560.22	999.71	14.04	53.97	127.47	147.42
Andrea	0.00	2010.12	6.75	7.92	0.09	295.59	386.90	1101.62	0.00	36.73	146.94	169.56
Tercer Cielo	0.00	2702.86	9.04	7.19	0.07	401.91	412.12	1530.23	0.00	52.06	198.15	177.68
Tankah Road	0.00	3004.13	10.31	9.15	0.11	454.57	745.34	1780.00	0.00	58.25	222.54	189.76
Tankah Cenote	0.00	2928.76	9.94	6.92	0.09	441.98	643.99	1694.53	0.00	57.25	218.73	189.07
Encantado	0.00	2940.44	10.25	5.54	0.11	441.97	405.02	1703.26	0.00	58.68	216.08	184.70
Tankah (Caleta)	0.00	5324.69	17.84	6.19	0.07	781.33	837.22	3097.16	0.00	105.62	385.86	227.09

Table 2 (continued)

ID	Fluoride	Chloride	Bromide	Nitrate	Phosphate	Sulfate	HCO3	Sodium	Ammonium	Potassium	Magnesium	Calcium
Outlet 1.2	0.00	8231.65	30.50	4.17	0.04	1326.58	2193.42	5171.23	0.00	179.71	639.36	281.80
Outlet 1.1	0.00	9438.22	36.02	13.64	0.05	1582.79	3219.74	6181.50	0.00	215.15	763.93	308.10
Azulik Beach	0.00	16717.06	56.64	27.28	0.02	2546.51	2296.03	9982.78	0.00	344.74	1236.12	371.95

temporal variation between 2016 and 2017, and the lower concentration trend can be attributed to three main factors:

- Sampling in cenote in 2017 was deeper than in 2016; therefore, samples were probably less impacted by anthropic influence.
- Improvement in waste water management over the study area in general and in Tulum city in particular (better connection to the municipal wastewater treatment plant)
- In 2017, incubation of our samples has suffered from numerous power cut-offs that might have impacted bacterial growth

Analysis in Grand cenote provides an evidence of contamination by tourism as *E. coli* concentrations varies from 0 CFU/100 ml at entrance to a TNTC result at exit (Fig. 3). Contamination is probably due to dry toilets that are set up near touristic cenotes with potential leakages directly in conduits. These cenotes results point out potential problems regarding the use of cenotes for leisure activities as they are a part of the karstic system that feeds the whole area with fresh water. Even though the city water company (CAPA) is pumping water upstream from the touristic cenotes on northern corner of the study area (city's wells are identified as CAPA 7, 5 and 3), remotes houses that are not connected rely on wells that are possibly downstream of these touristic places.

Results in outlets 1.1 and 1.2 (Fig. 3) emphasize another problem of water management in karstic environment: the very high variability of contamination between two conduits that are extremely close to one another. Outlet 1.2 shows no contamination, whereas samples of outlet 1.1 provide us with a mat of *E. coli* bacteria that is considered to be too numerous to count (TNTC). These outlets are both at the same distance from the beach and are only 50 m away from each other. Sea water mixing is more important in 1.1 than in 1.2 (concentrations of chloride, sodium, sulfate, potassium and magnesium are lower in 1.2), so dilution of contaminants like *E. coli* bacteria is more important in 1.1, nevertheless *E. coli* contamination remains higher in 1.1 (TNTC). We can exclude a contamination during sampling, as outlet 1.1 has been sampled 10 mn before 1.2; furthermore *E. coli* results of these outlets have been correlated by nitrate results (higher concentration in 1.1 than in 1.2, respectively, 13.6 mg/l and 4.2 mg/l). These differences between two close sampling points demonstrate the complexity of establishing a reliable contamination map for a contaminant introduced in specific points of a karstic network.

(a) *E. coli* concentrations are correlated with human activities, leisure activities like in Gran Cenote exit which is clearly contaminated by tourists, or daily life activities like in TU8 which is used as a sewage. Nevertheless,

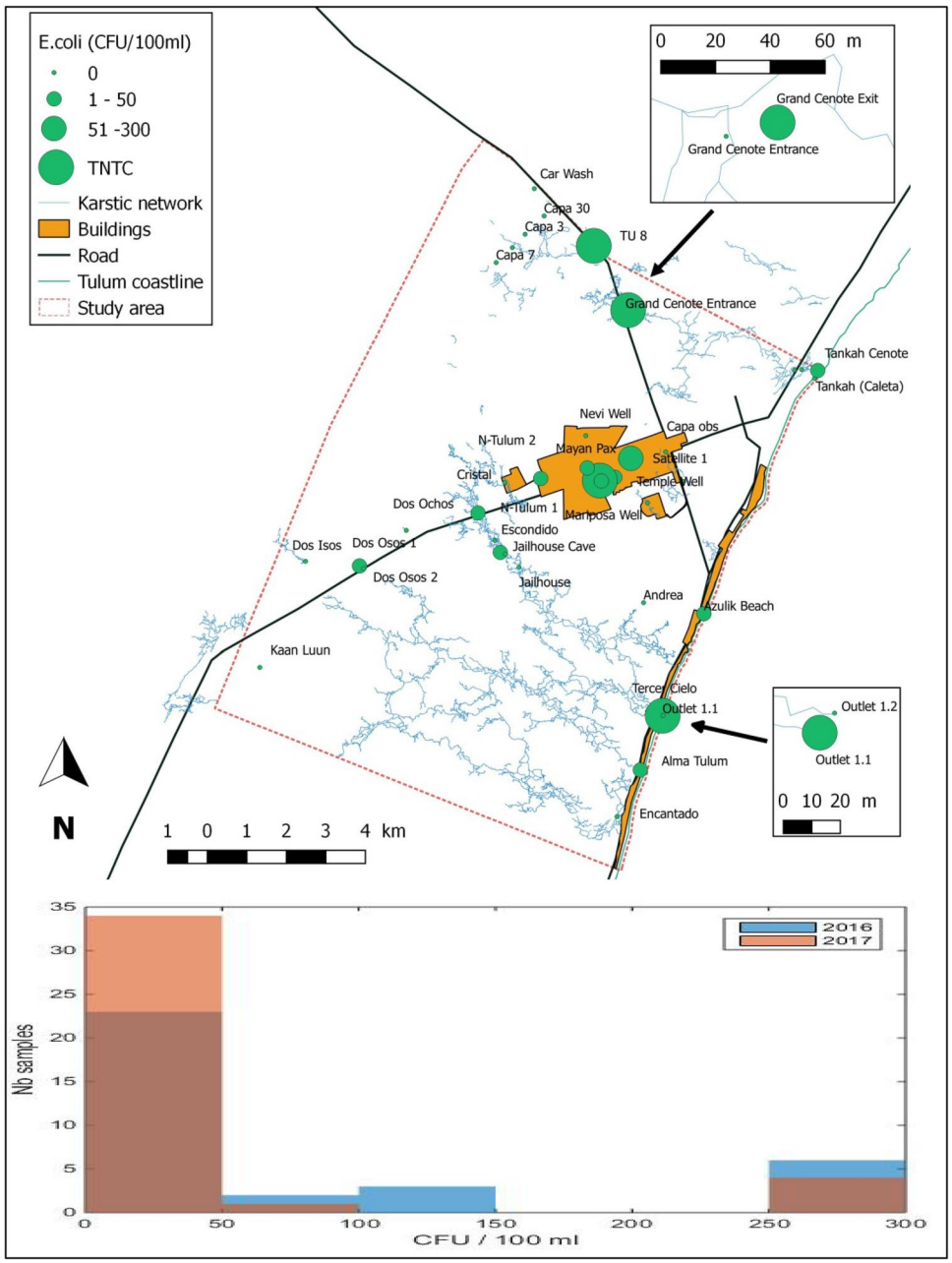

Fig. 3 Map of *E. coli* 2017 concentrations in CFU/100 ml and distribution of *E. coli* concentrations in 2016 (blue) and 2017 (brown). Inset zooms in **a** represent entrance and exit of Gran Cenote and outlets 1.1 and 1.2. Vertical axis in **b** indicates the number of samples

Ak Tulum shows an enhancement of water quality due to the cleaning of the area as results were too numerous to count in 2016 and no contamination occurs in 2017 (Electronic supplement material 10).

Major ions

The piper diagram (Fig. 4) provides us with an overview of the groundwater characteristics within the study area. Two main trends are displayed; samples from Caribbean Sea, outlets and cenotes contain sodium chloride, whereas samples from wells correspond to calcium bicarbonate.

Total dissolved solid (TDS) values vary from 559.79 mg/l in Well Front Mariposa to 33579.10 mg/l in Azulik beach, box plots (Fig. 5) illustrate differences between wells, cenotes, outlets and sea. The horizontal red line corresponds to the 1000 mg/l concentration limit of Mexican norm (NOM-127-SSA1-1994) for drinkable water and shows that most of the samples (85%) are above that limit.

Total alkalinity (TAC) is approximated to $HCO3^-$ concentration. Values vary from 231.8 mg/l in Kaan Luum which corresponds to the inland limit of the study area to 560.22 mg/l in Alma Tulum (measured values) which is a hotel located on Caribbean coast. The calculated value in

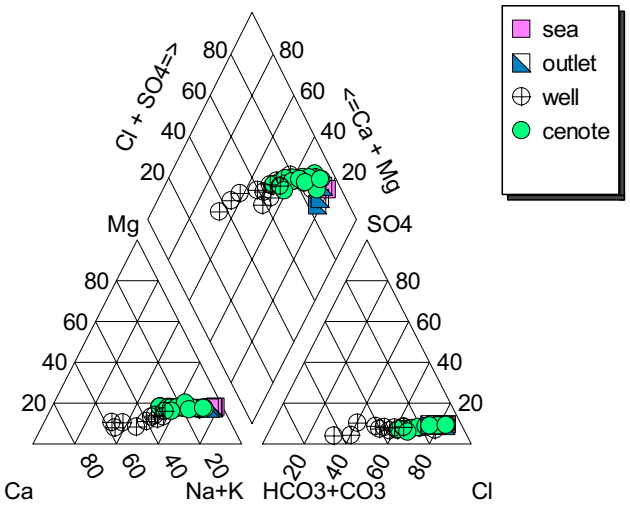

Fig. 4 Piper diagram of samples clustered in four groups, sea, outlet, well and cenote

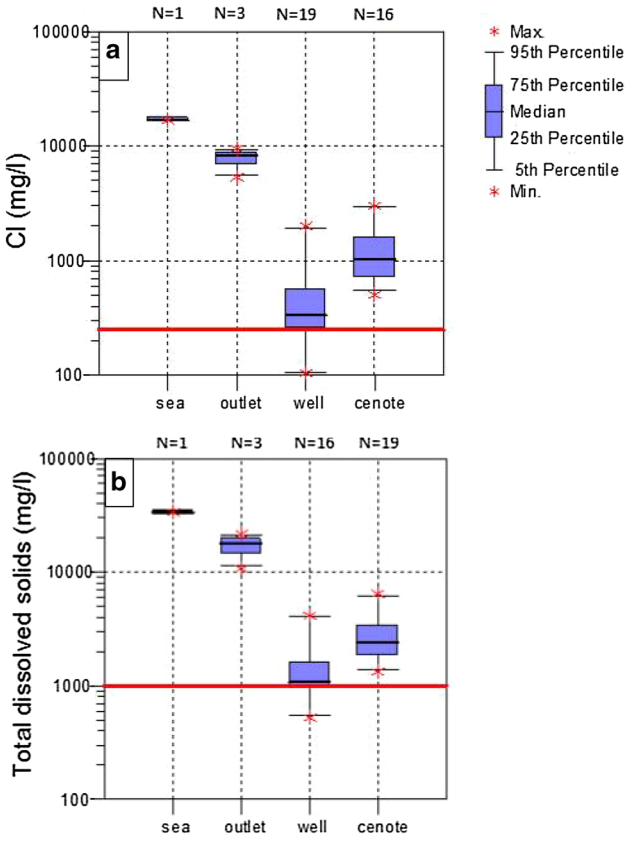

Fig. 5 Distribution of chloride (**a**) and TDS concentrations (**b**) (mg/l), red line corresponds to Mexican norm for drinkable water (NOM-127-SSA1-1994). Both distributions follow the same trends as concentrations in wells are lower than in other group of sampling sites

Outlet 1.1 (coastal outlet) reaches 3219 mg/l. Nitrite, lithium, and strontium have not been detected.

Positions of wells in the Piper diagram indicate that they are less influenced by seawater mixing than cenotes. As an example, samples N Tulum 1 and 2 were made in a well and in a cenote, respectively, even though only 20 m separate both sites; N Tulum 2 is slightly more on the sodium chloride type than N Tulum 1. This could be explained by conduits that provide a better connection with sea due to a higher hydraulic conductivity than matrix where wells can be dug.

Ions are clustered in two groups:

- Seawater contribution: chloride, sulfate, bromide, sodium, magnesium, potassium and calcium
- Inland contribution (anthropic and natural): ammonium, nitrite, nitrate, phosphate and fluoride

Seawater contribution

Chloride (Cl^-) The general trend for chloride ions is a decreasing concentration when the distance from the coast increases. This can be explained by the progressive deepening of the mixing zone correlated with the distance from the coast (Bauer-Gottwein et al. 2011).

Chloride concentrations are lower in wells than in cenotes, outlets or sea (Fig. 5). The red horizontal line illustrates the WHO guidelines of 250 mg/l for chloride concentration in drinkable water, 92% of samples have a higher chloride concentration.

Chloride map (Fig. 6) points out that the Tulum city center is not following this general trend, as the chloride concentrations are very low compared to samples taken at the same distance from the coast. Samples in the Tulum city centers are taken from wells and piezometers, in the vicinity of Tulum, as well as from cenotes and conduits. As seen with the piper diagram, sampling sites with higher conductivity (cenotes and conduits) display a higher chloride concentration than wells. Wicks and Herman have attempted to model a FWL in coastal karst aquifer and found out that: "the effect of cavernous porosity is to decrease the volume of aquifer in which freshwater occurs", particularly if the high permeability zone is located at a shallow depth. A previous study pointed out that the depth of the halocline was deeper in hand-dug wells than in conduit sites (Beddows et al. 2007). At the moment, no conduits are mapped under the Tulum city center, but a thicker FWL could occur under the Tulum city center resulting in a deeper mixing zone and therefore, a lower chloride concentration at shallow depth. Andrea's well value is explained by the fact that it is mapped over a conduit.

The Pleistocene limestone deposits are divided into lower, middle and upper Pleistocene, each unit is capped

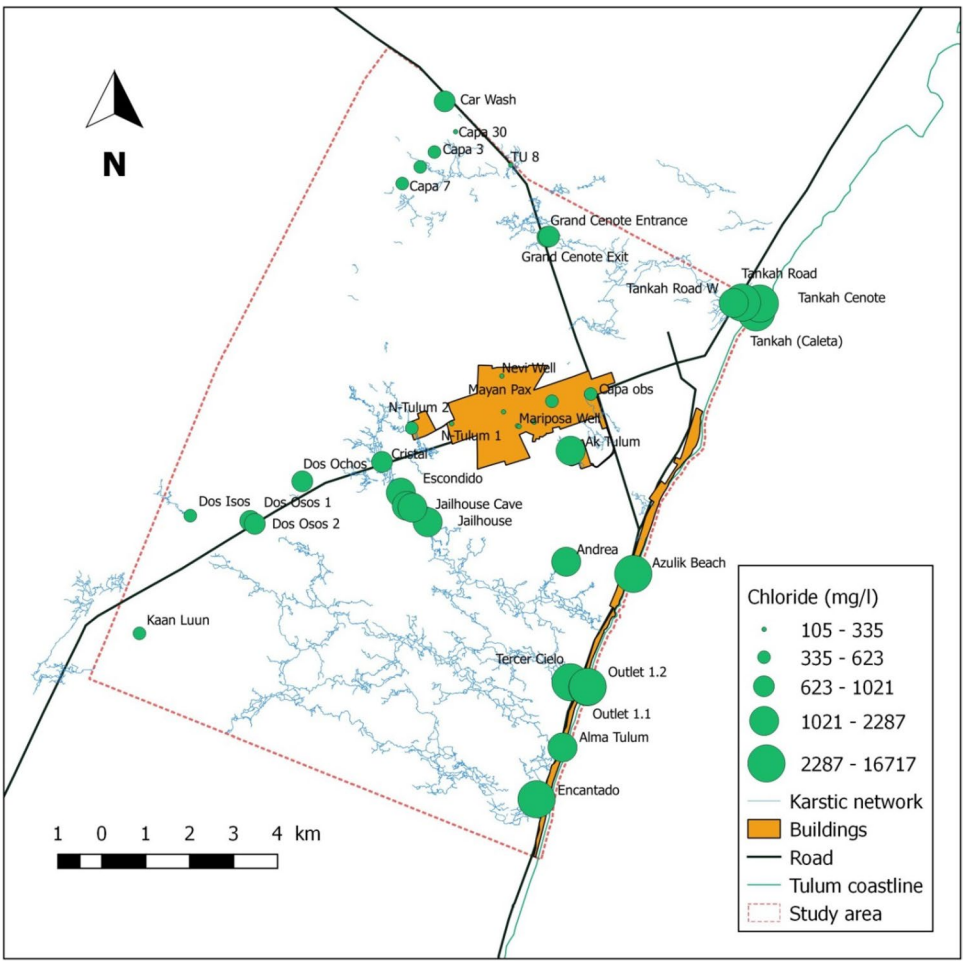

Fig. 6 Map of chloride concentration (mg/l), values in the Tulum city center are particularly low compared to sites at the same distance from the coast

by a zone of calichification (Ward 2003); a lower conductivity could result from a caliche lens in the vicinity of Tulum.

Chloride value in CAPA 3, 5 and 7 (inland border of the study area) are higher (538, 531 and 620 mg/l) than in CAPA 30 (106.35 mg/l) which is a piezometer; this implies that samplings have been made deeper in the three wells than in the piezometer (top of the water table). This difference is correlated by studies of the conductivity gradient in the water column of YP aquifer (Beddows et al. 2007). A similar chloride gradient is measured between Jailhouse and Jailhouse cave, respectively, 1096 mg/l and 1450 mg/l. These two samples are in the same system (Naranjal), 20 m one from the other, Jailhouse cave being 10 m deeper than Jailhouse. Even near the top of the water table, a chloride gradient is noticeable, therefore; a thicker freshwater lens would lead to lower chloride value in the Tulum city center wells.

The hypothesis of low chloride values in town due to leakage of freshwater from CAPA's supply network is in contradiction to the higher chloride concentration in upstream CAPA's wells. These concentrations should be then at least equal in the Tulum city.

Two main parameters seem to drive the depth of the mixing zone and thus chloride concentration in samples, distance to the coast of sampling sites and hydraulic conductivity of the sampling area.

A lower hydraulic conductivity in the area of the Tulum city center would produce higher water levels. Arnulf Schiller from Geological Survey of Austria (GSA) provided us with water level measurements made in 2012. Figure 1 displays the values obtained after kriging over the study area. It shows a zone of high water levels around Tulum that could correlate with the low hydraulic conductivity and thus lead to a thicker FWL and a deeper halocline.

The general trend for chloride concentration is to rise while approaching the coast, higher concentrations are found in locations like Tankah cenote or Tercer cielo (Electronic supplement material 12) which are less than 100 m from the coast. Nevertheless, sampling locations in the city center show lower concentrations compared to their distance to the coast, this might be due to geologic heterogeneities.

Bromide (Br^-) Cl/Br ratio (in weight) is used to trace the origin of water (Vengosh and Pankratov 1998). A ratio of 297

corresponds to seawater (ratio is 295.16 in Azulik beach). In their study, Vengosh and Pankratov obtained for uncontaminated ground water a range of ratios from 173 to 293 and for contaminated groundwater a range of ratios from 150 to 540. Coastal samples are close to seawater ratio; the values of these ratios then increase in anthropized places. Touristic cenotes like Dos Isos or Gran Cenote and urbanized area especially like the Tulum city center have ratio values corresponding to sewage-contaminated water (Table). Inset zoom in Electronic supplement material 2 shows the impact of leisure activities on cenotes, Jailhouse cave, which is a conduit, shows a much lower ratio than cenotes located upstream and downstream, whereas these sampling points are in the same karstic network (Naranjal).

The city center shows a low chloride concentration as noted above, while the high Cl/Br ratio indicates that a part of this chloride concentration comes from sewage contamination, thus this results indicates a much lower influence of sea water intrusion in the Tulum city center than in other places located at the same distance from the coast.

Table 3 Chloride/Bromide ratios show values of the three last samples that are below 300, all others are over 316 which indicate a possible contamination

Samples	Cl/Br ratio
Dos Isos	321.44
Grand Cenote exit	316.16
Temple Well	337.04
Mayan Pax	346.06
Nevi Well	339.66
Mariposa Well	342.64
Outlet 1.2	269.85
Outlet 1.1	262.04
Azulik Beach	295.16

Cl/Br ratios show that groundwater is more contaminated in the city center and touristic places compared to remote areas. It highlights the anthropic impact and the needs in terms of wastewater management (Table 3).

Sodium (Na^{+}), magnesium (Mg2+), potassium (K+), sulfate ($SO4^{2-}$) Plots of chloride versus sodium, magnesium, potassium and sulfate show good correlations, respectively, 0.999, 0.999, 0.997 and 0.998 (Electronic supplement material 11) which indicates a seawater origin for these ions. The seawater origin of ion indicates that groundwater flow through evaporites or rocks like dolomite ($CaMgCO_3$) may occur, but with almost no impact on water chemistry.

Calcium (Ca^{2+}) Calcium concentration shows a correlation of 0.93 with chloride. Most of cenotes and conduits are on a line corresponding to seawater mixing (Fig. 7). A group of wells have calcium concentrations between 82.45 mg/l (CAPA 30) and 117.08 mg/l (N Tulum 1) but, in these cases, increasing calcium concentrations are not correlated with an increase of chloride concentrations, these value correspond to wells in the Tulum city center (Electronic supplement material 12) that have been pointed out above for their low chloride concentration. Mean SI values for calcite and aragonite are, respectively, 0.17 and 0.02 (Electronic supplement material 14) If we consider only wells located in the city center, SI mean value for calcite and aragonite are, respectively, 0.01 and −0.01. SI is higher in samples with a higher chloride concentration, whereas seawater mixing should lower SI and thus increase calcite dissolution and Ca^{2+} concentration. We can therefore consider that variation of calcium concentration between the Tulum city center and the rest of the field is not due to SI variations. These calcium values could be due to upstream calcite dissolution, they are

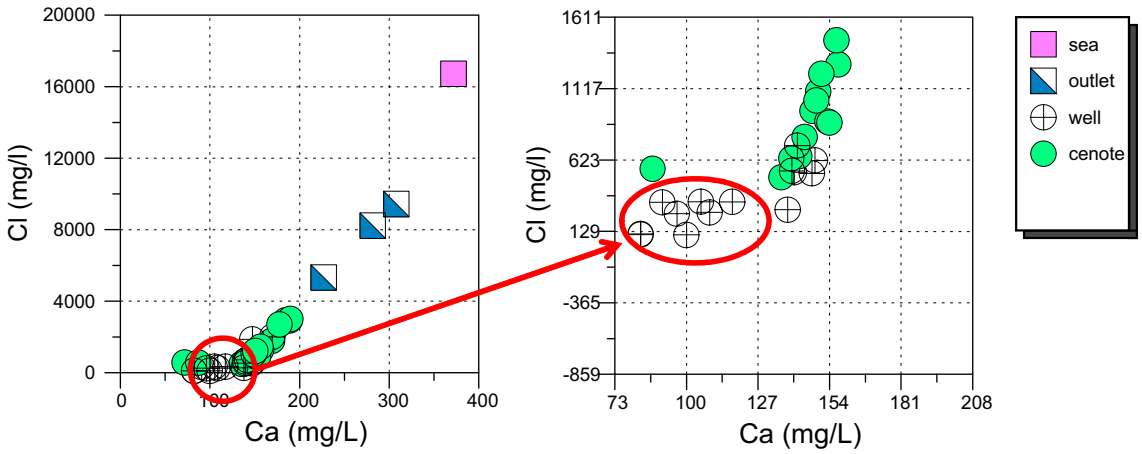

Fig. 7 Correlation between chloride and calcium, wells located in the city center are not on the seawater mixing line (red circle)

not or only lightly influenced by seawater mixing. Concentrations outlined by red circles in Fig. 7 may represent the inland input of calcium.

The calcium concentrations are highly influenced by seawater input, the lower calcium concentrations in the Tulum city center indicate that there is probably a lower rate of seawater mixing in the city center area.

Cl/Na The Cl/Na molar ratio varies from 0.98 for outlet 1.1–1.59 in cenote Jailhouse. Perry et al. (2009) provides a Cl/Na ratio of 1.17 for seawater dilution and 1 for halite dissolution as a source of ions.

During upper Pleistocene (120,000 YBP), maximum highstand was approximately 6 m above the present sea level (Rohling et al. 1998). Elevation corresponding to 6 m is shown in Electronic supplement material 4. As mentioned above, the upper Pleistocene deposits correspond to lagoon limestone. A lagoon depositional environment is subject to high rate of evaporation and evaporites deposit. Lens of evaporites could explain ratios close to 1 found near the coast.

Inland contribution (natural or anthropic)

Ammonium (NH^{4+}) Ammonium is present in the anaerobic environment and is mainly due to degradation of organic matter; it is therefore detectable mainly in wells (Electronic material supplement 5). Few cenotes are also contaminated with ammonium (Dos Isos, Dos Osos), this can be explained by stagnant water. Jailhouse cave's NH^{4+} concentration illustrates the fact that when in contact with atmosphere, ammonium gets oxidized (Electronic supplement material 6) and turns to nitrate. Cristal, Escondido, Juan Cenote, Jailhouse cave and Jailhouse are part of the same system (Naranjal), only Jailhouse cave were sampled in a conduit; the four others were sampled in cenotes and show no ammonium concentration.

Ammonium concentrations indicate the oxidation state of waters, when samples are made in stagnant waters or in location with no direct access to atmosphere, ammonium concentrations are higher.

Nitrites (NO_2^-) and nitrates (NO_3^-) The lack of nitrite is explained by its instability; it quickly turns to nitrate during the denitrification process. Nitrate concentrations vary within the study area from 0.3 to 28.5 mg/l, without correlation or inverse correlation with chloride (Electronic supplement material 15). Concentrations of ammonium obtained upstream of Tulum are in the same range as those obtained in city center (mean ammonium concentration for CAPA and Tulum samples are, respectively, 1.58 mg/l and 2.35 mg/l). There is no inverse correlation between ammonium and nitrate (Electronic supplement material 15); therefore, oxidation of ammonium cannot explain concentrations of nitrates observed. Higher values correspond to anthropized areas like the Tulum city center or hotels and touristic cenotes like Grand cenote, this points out the human impact on water quality.

Like for *E. coli*, samples' results confirm the high variability of values that can be obtained over an area. The outlets 1.1 and 1.2 show values of, respectively, 13.6 mg/l and 4.2 mg/l even though barely 50 m separate both places. Mariposa well and Well Front Mariposa have concentrations of, respectively, 7.5 mg/l and 12.1 mg/l even though it is only 40 m from one to the other (Fig. 8). It is interesting to note that for outlets 1.1 and 1.2 on one hand and for Mariposa Well and Well Front Mariposa on the other hand, values of *E. coli*, as values of nitrates of both couples of data are in the same range. Furthermore, when nitrate values are approximately doubled, values of *E. coli* vary from 0 to 20 CFU/100 ml to a result considered as TNTC. The above findings and the almost lack of agriculture tend to confirm the wastewater origin of nitrates.

Nitrate concentrations are due to human activities (waste waters) as higher values correspond to water samples taken in the city center area or touristic cenotes.

Fluoride (F^-) Only 7 out of 39 samples present a contamination of fluoride, all in the urbanized area, only one of these 7 samples (Alma Tulum) is located out of the city center (Electronic supplement material 7). As fluoride can precipitate with calcium as fluorite mineral (Eq. 4), saturation index has been calculated with respect to fluorite (Electronic supplement material 14) and the results indicate that all the study areas are undersaturated with respect to fluorite (higher SI value is -1.55 for Alma Tulum), meaning that no fluorite precipitation occurs. Low Ca^{2+} concentrations in city center's wells (Electronic supplement material 8) may explain the subsaturation state, where the fluoride concentration is higher, Ca^{2+} concentration could be in these cases the limiting factor for fluorite precipitation leading to a higher fluoride concentration in solutions.

$$CaF_2(s) \leftrightarrow Ca^{2+}(aq) + 2F^-(aq) \quad (4)$$

Nevertheless, even if the water is undersaturated with respect to fluorite (i.e., $SI_{Fluorite} < 0$), adsorption on calcite removes fluoride (Turner et al. 2005) and this process controls the fluoride concentration in our samplings over our study area except in the city center's wells and Alma Tulum's well. It can be explained by anthropic inputs like fertilizers (Fluorapatite) on hotel lawns or herbicides. All measured values were below the WHO guideline (2003) of 1.5 mg.l.

Fluoride concentrations are due to human activities, higher concentrations correspond to several wells in the

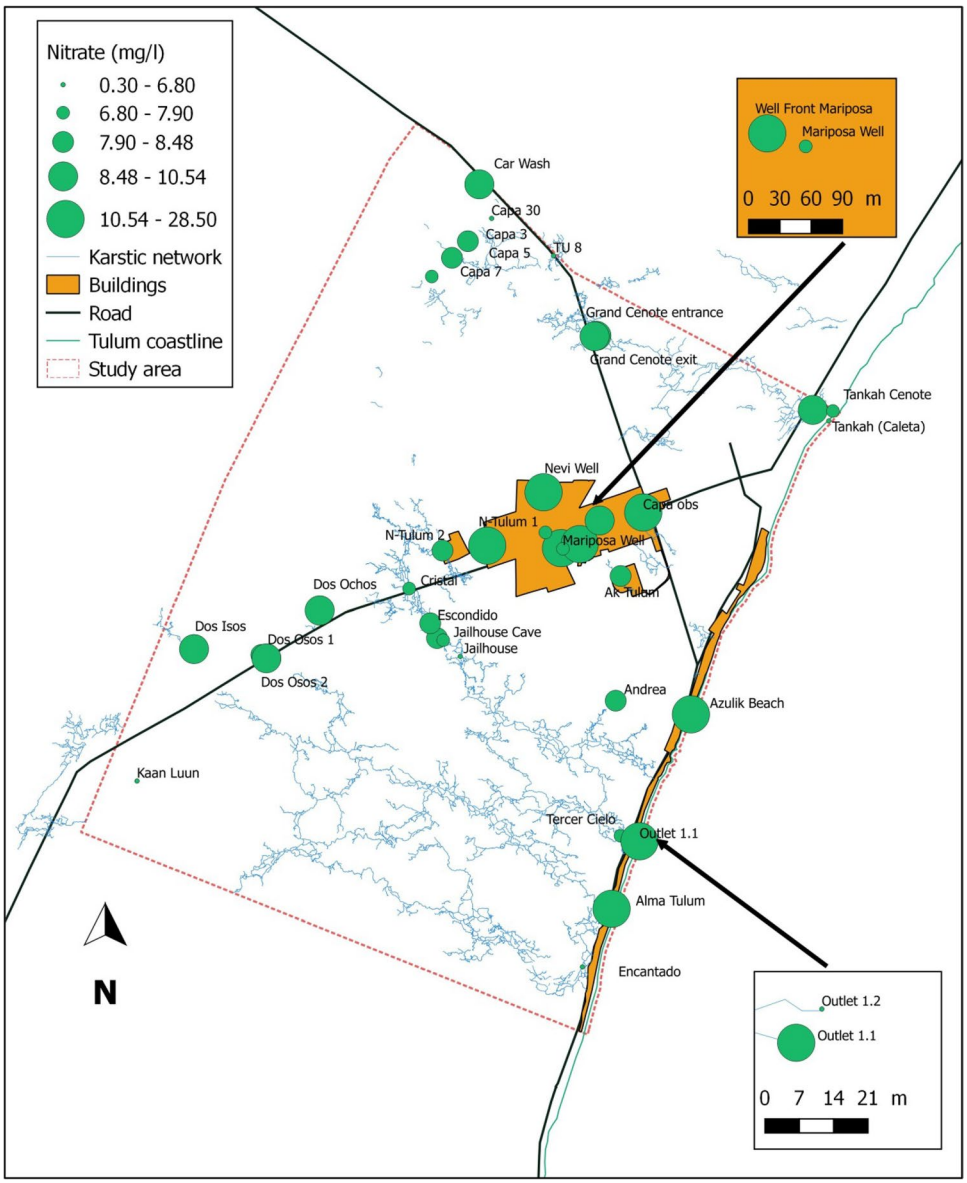

Fig. 8 Map of nitrate concentrations, inset zoom highlights the spatial variability of results

city center and a hotel (Alma Tulum); it can be explained by the use of fertilizers like fluorapatite.

Phosphates ($PO4^{3-}$) Phosphates have four main origins, agriculture, industrial and domestic wastes (as detergents) and human excrements. The box plot (Electronic supplement material 9) shows homogeneous phosphate concentrations within the study area only disrupted by results corresponding to wells in the Tulum city center (Fig. 9), even though results within the city center are variable, concentration of phosphates vary from 0.01 to 1.54 mg/l. TU8 is remote from city center but during the sampling session, we noticed that the piezometer cap was broken and the smell was very bad, we therefore can believe that it is used as sewage and thus affected by human activities. The high concentrations of phosphate obtained in city center lead to exclusion of agriculture as an origin of phosphate peaks.

As nitrates in the aquifer are a result of septic tank leakage, the lack of correlation between phosphates and nitrates (-1.7×10^{-2}) would then exclude human excrement as an origin for phosphates.

Phosphates in karstic environment can precipitate as hydroxyapatite, a saturation index has been calculated with respect to hydroxyapatite ($Ca_5(PO_4)_{3)}$, the only positive result is in TU8 (1.761), all others samples are undersaturated with respect to hydroxyapatite. The value in TU8 confirms the use of this piezometer as sewage, undersaturation in other sites indicates that no precipitation of hydroxyapatite occurs. PO4 adsorption and desorption by calcium carbonates is nevertheless a prominent process for control of phosphate's concentration in karstic aquifer

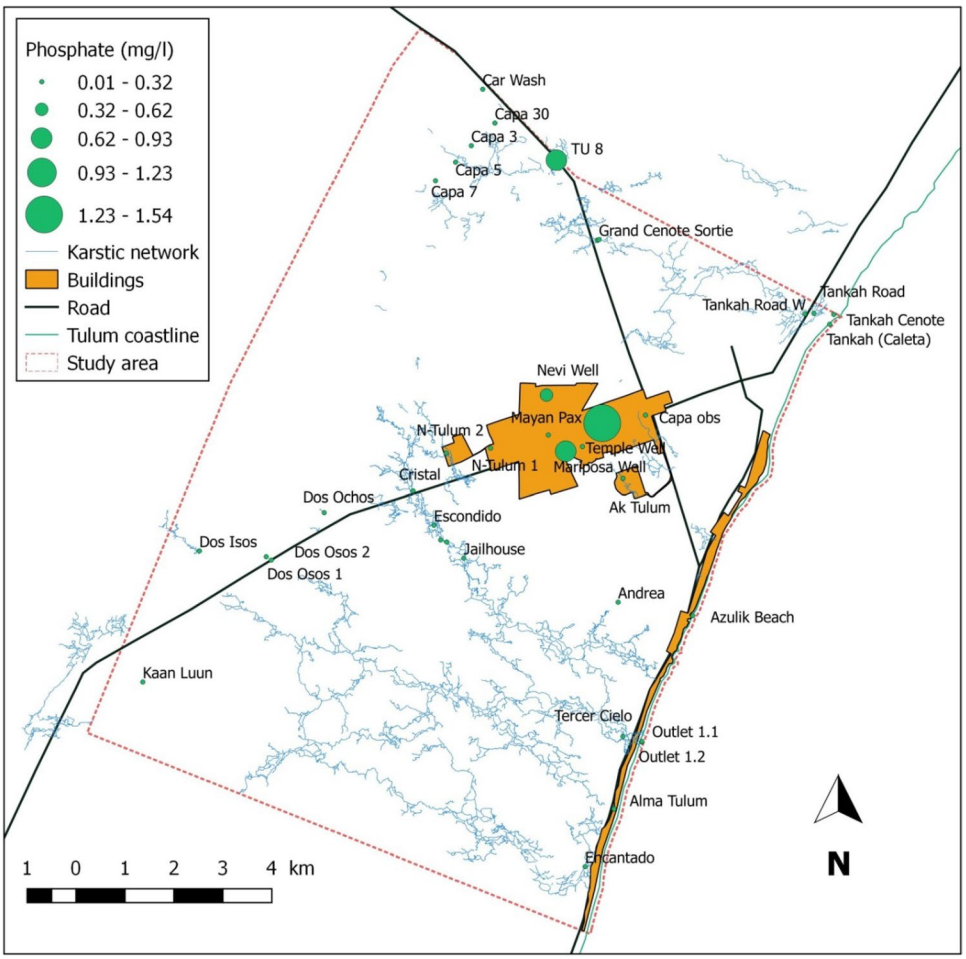

Fig. 9 Phosphate concentration map, sampling sites in the city center displays higher values, TU8 is remote from the city but it is probably used as a sewage considering the bad smell of the samples

(Millero et al. 2001). A saline intrusion diminishes the adsorption compared to a freshwater input mainly due to lowered HCO_3^- concentration. The Tulum city center present in the same time a low chloride and bicarbonate concentration (which means adsorption process is efficient) and a higher phosphate concentration. This indicates that the peaks of phosphate concentrations are due to localized anthropic input and not to geological heterogeneities (Table 4).

Furthermore, samples made in CAPA wells (which are at the inland border of the study area) show a mean concentration of 0.075 mg/l (these wells provide the city center of Tulum with fresh water) and the mean value for phosphate concentration in the study area is 0.084 mg (standard deviation = 0.28). The origin of phosphate peaks are four localized sites in Tulum (TU8, Satellite 1, Mariposa Well and Navi Well). If we exclude the values of these four sites, the mean value becomes 0.065 mg/l (standard deviation = 0.05) which is slightly below CAPA's wells mean values. This means that there is no widespread addition of phosphates, but only local injections probably due to detergent and washing powder.

Phosphate concentrations are due to localized anthropic input in wells that are used as raw sewage, mainly in the Tulum city center.

Isotopes

Delta ^{18}O vs delta ^{2}H

Figure 10 shows that samples follow two main trends, the wells' group is lightly influenced by seawater mixing, whereas cenotes', outlets' and sea groups are much more influenced by seawater mixing. Cenote linear regression (red dashed line) corresponds to seawater mixing line (Fig. 10). Kaan Luum sample shows a different behavior compared to other cenotes, this sampling site is a wide lagoon and thus is subject to a high rate of evaporation compared to smaller cenotes in the forest, nevertheless, Fig. 10b shows that this lagoon (red circle) is only very lightly influenced by seawater mixing. CAPA 30 is also very lightly influenced by seawater mixing (chloride concentration is very low), but this site is not subject to such evaporation rates like Kaan Luum as it is a piezometer. The slope of the well's linear

Table 4 Saturation index (SI)

ID	SI anhydrite	SI aragonite	SI calcite	SI dolomite	SI fluorite	SI gypsum	SI halite	SI hydroxapathite
Ak Tulum	−1.51	−0.33	−0.188	−0.2		−1.27	−4.44	−3.78
Alma Tulum	−1.66	0.12	0.27	0.77	−1.55	−1.43	−4.41	−2.19
Andrea	−1.49	−0.4	−0.24	−0.25		−1.26	−4.34	−4.72
Azulik Beach	−0.91	1.73	1.87	4.61		−0.69	−2.59	−1.43
Capa 3	−1.88	−0.37	−0.22	−0.59		−1.64	−5.44	−4.88
Capa 30	−2.58	−0.38	−0.22	−1.26		−2.35	−6.8	−3.87
Capa 5	−1.88	0	0.15	0.15		−1.64	−5.44	−3.21
Capa 7	−1.83	−0.04	0.1	0.07		−1.59	−5.32	−3.25
Capa obs	−2.09	−0.05	0.1	−0.18		−1.86	−5.81	−2.68
Car wash	−1.81	−0.24	−0.1	−0.28		−1.58	−5.28	−5.98
Cristal	−1.69	−0.26	−0.11	−0.2		−1.45	−4.95	−4.31
Dos Isos	−1.9	0.21	0.36	0.57		−1.66	−5.49	−1.95
Dos Ochos	−1.76	−0.13	0.01	−0.02		−1.52	−5.12	−4.08
Dos Osos 1	−1.82	0.18	0.33	0.56		−1.59	−5.3	−2.47
Dos Osos 2	−1.78	−0.08	0.06	0.06		−1.54	−5.2	−2.75
Encantado	−1.4	−0.17	−0.02	0.33		−1.16	−4.01	−3.52
Escondido	−1.61	−1.61	−0.07	−0.03		−1.37	−4.7	−7.11
Gran Cenote entrance	−1.7	−0.06	0.09	0.15		−1.46	−5.02	−3.63
Gran Cenote exit	−1.7	−0.01	0.13	0.24		−1.46	−5.03	−3.42
Jailhouse	−1.66	0.13	0.27	0.6		−1.42	−4.84	−3.09
Jailhouse Cave	−1.58	−0.44	−0.29	−0.44		−1.34	−4.61	−6.07
Juan Cenote	−1.68	−0.18	−0.04	−0.03		−1.44	−4.88	−6.57
Kaan Luun	−2.07	0.37	0.52	1.18		−1.83	−5.38	−0.33
Mariposa Well	−2.07	−0.25	−0.11	−0.51	−1.66	−1.84	−5.82	−0.11
Mayan Pax	−2.04	−0.12	0.03	−0.44	−2.3	−1.81	−6.01	−1.52
Nevi Well	−1.97	−0.37	−0.23	−1.13		−1.73	−5.98	−2.09
N Tulum 1	−1.99	0	0.15	−0.07		−1.75	−5.83	−2.58
N Tulum 2	−2.06					−1.82	−5.5	−2.67
Outlet 1.1	−1.06	0.97	1.12	2.95		−0.83	−3.03	−3.78
Outlet 1.2	−1.11	0.62	0.77	2.21		−0.88	−3.15	−4.85
Satellite 1	−1.82	0.38	0.53	0.87	−1.91	−1.58	−5.41	2.74
Tankah Caleta	−1.25	0.19	0.33	1.2		−1.02	−3.53	−4.06
Tankah Cenote	−1.4	0.04	0.18	0.73		−1.16	−4.02	−3.77
Tankah Road	−1.4	0.15	0.3	0.97		−1.16	−3.99	−3.25
Tankah Road West	−1.61	−0.04	0.1	0.28		−1.38	−4.74	−2.72
Temple Well	−2.05	−0.02	0.13	−0.06	−1.91	−1.81	−5.99	−2.11
Tercer Cielo	−1.43	−0.23	−0.08	0.18		−1.19	−4.09	−4.43
TU 8	−2.49	0.23	0.38	0.09	−2.54	−2.26	−6.76	1.76
Well Front Mariposa	−2.2	0	0.15	−0.34	−1.92	−1.97	−6.72	−0.07

regression (blue line) varies slightly from the slope of Veracruz meteoric water line (Fig. 10a), and its equation is: $y = 7.19x + 6.95$. This shift can be due to exchange with H_2S as wells are mostly anaerobic environments as shown with ammonium concentrations.

Isotope ratios $^{2}H/^{18}O$ indicate that wells are less influenced by seawater mixing than cenotes and conduits which can be explained by the facts that wells are dug in a calcareous matrix with lower hydraulic conductivity than conduits (Table 5).

Discussion

The results of *E. coli*, major ions and isotopes analysis provide a snapshot of the groundwater quality. It helps to identify the origin of solute contaminants and bacteria.

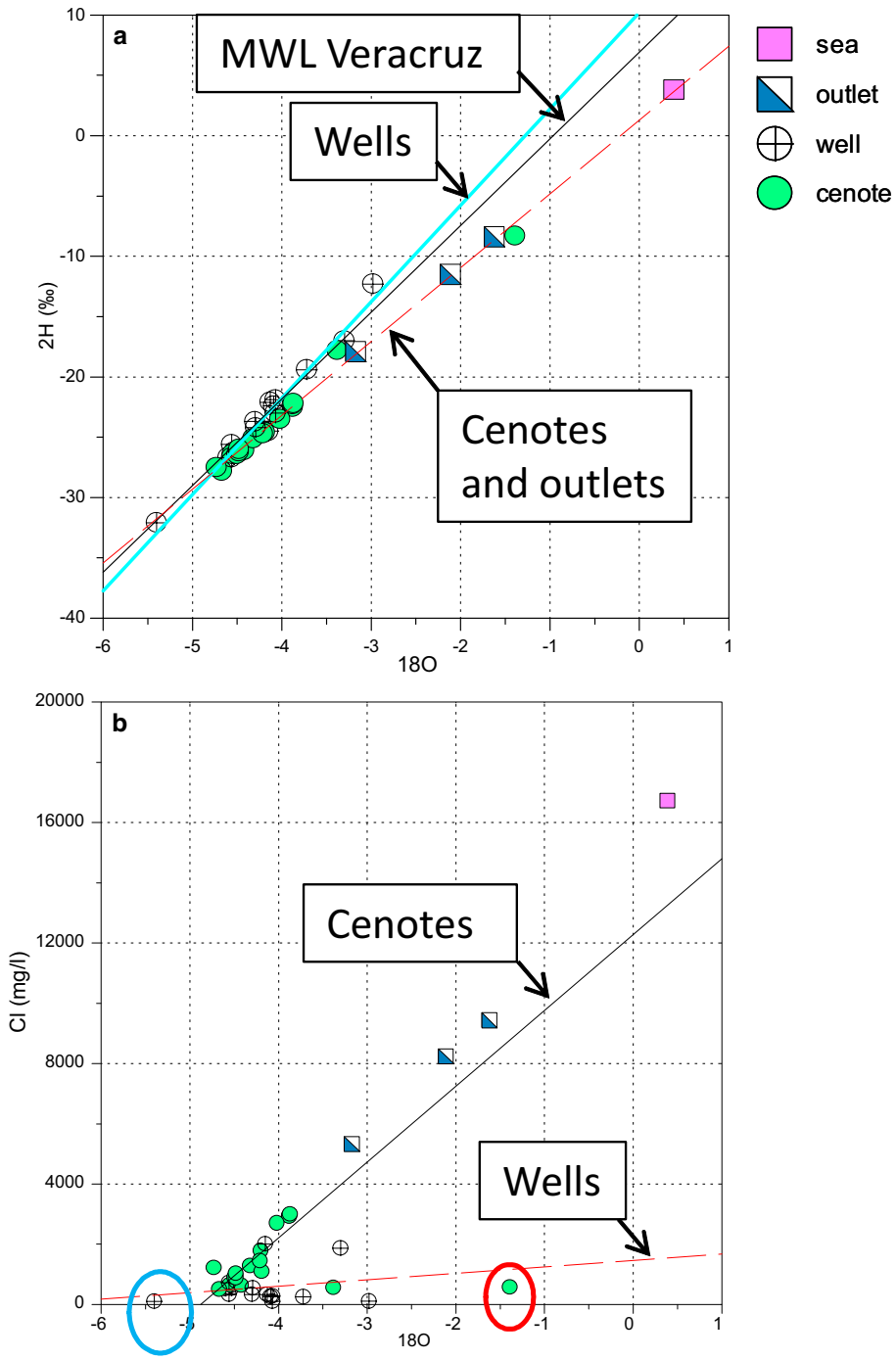

Fig. 10 Scatter plot **a** shows samples of cenotes, conduits and outlets that are on the seawater mixing line (red dashed line) whereas wells' regression line is closer to Veracruz meteoric water line. The red dashed line corresponds to sea evaporation and mixing of seawater with groundwater. On scatter plot **b**, wells' linear regression (red dashed line) show the lower influence of seawater mixing compared to cenotes' regression line. Kaan Luum (red circle) is very lightly influenced by seawater mixing but subject to a high rate of evaporation; CAPA 30 (blue circle) is lightly influenced by seawater mixing and not subject to evaporation

It appears that groundwater is considered as non-drinkable in 85–92% of the samples as they exceed the NOM-127-SSA1-1994 limit for, respectively, TDS and chloride concentration, this is mainly due to the seawater intrusion. The Tulum city center seems to be less subject to seawater intrusion, possibly due to a lower conductivity compared to the rest of the study area.

Nevertheless, the peaks of fluoride, nitrate and phosphate concentrations are correlated with human activities and thus, even if the concentrations are not alarming, they need to be surveyed considering the city development.

Escherichia coli results indicate that fecal contamination remains a major issue in and around Tulum as the presence of *E. coli* makes GW non-drinkable. The higher concentrations found in the city center point out the needs in terms of wastewater management. Samples collected in 2017 show a lower concentration of *E. coli* compared to those collected in 2016, this could be a positive sign.

Table 5 Isotopes table for deuterium and 18O

ID	δ2H, in ‰	δ2H Std. dev., in ‰	δ18O, in ‰	δ18O Std. dev., in ‰
Capa 30	−32.1	0.43	−5.4	0.03
Well Front Mariposa	−12.3	0.16	−2.98	0.02
TU 8	−23	0.1	−4.07	0.02
Mayan Pax	−22.4	0.09	−4.09	0.02
Temple Well	−19.4	0.07	−3.72	0.02
Nevi Well	−21.9	0.08	−4.07	0.02
Mariposa Well	−22.1	0.05	−4.13	0.02
Capa Obs	−25.6	0.07	−4.56	0.03
N Tulum 1	−23.7	0.06	−4.3	0.01
Kaan Luun	−8.3	0.16	−1.39	0.02
Dos Isos	−27.8	0.44	−4.67	0.04
N Tulum 2	−17.8	0.09	−3.38	0.01
Capa 5	−26.7	0.23	−4.6	0.03
Capa 3	−26.4	0.04	−4.53	0.01
Satellite 1	−24.2	0.07	−4.29	0.02
Dos Osos 1	−26.1	0.08	−4.42	0.02
Capa 7	−26.2	0.07	−4.53	0.03
Car Wash	−26.4	0.06	−4.55	0.03
Dos Osos 2	−26.7	0.06	−4.56	0.01
Dos Ochos	−26.3	0.07	−4.48	0.02
Grand Cenote exit	−26.2	0.42	−4.48	0.03
Grand Cenote entrance	−26.4	0.17	−4.5	0.01
Cristal	−26.1	0.12	−4.48	0.01
Juan Cenote	−26	0.13	−4.48	0.02
Jailhouse	−24.6	0.15	−4.19	0.04
Tankah Road W	−27.5	0.1	−4.73	0.02
Escondido	−25.1	0.13	−4.32	0.03
Jailhouse Cave	−24.7	0.15	−4.21	0.02
Ak Tulum	−24.5	0.05	−4.2	0.03
Alma Tulum	−17	0.17	−3.3	0.02
Andrea	−24.5	0.5	−4.15	0.05
Tercer Cielo	−23.5	0.14	−4.02	0.01
Tankah Road	−22.2	0.06	−3.87	0.01
Tankah Cenote	−22.3	0.06	−3.88	0.03
Encantado	−22.5	0.08	−3.88	0.02
Tankah (Caleta)	−17.9	0.08	−3.17	0.02
Outlet 1.2	−11.5	0.05	−2.11	0.02
Outlet 1.1	−8.4	0.13	−1.62	0.02
Azulik Beach	3.8	0.14	0.39	0.03

Nevertheless, Leal-Bautista et al. (2013) did a sampling campaign in the region of Tulum from 2008 to 2012 and *E. coli* bacteria was not detected in the samples collected in March and December (dry season), all samples indicating human fecal contamination were observed in July (wet season); our samples made in 2017 show contamination even during the dry season. Infiltration, hydraulic gradients, speed flow and thus residence time can vary depending on precipitations, we therefore think that an extensive sampling campaign would be necessary to provide reliable contamination map.

Conclusion

Escherichia coli results present a very high spatial variability which occurs even within very short distance, it highlights the difficulty of establishing a reliable pollution map. New accommodation complexes are planned in the vicinity of Tulum, whereas inhabitants already experience *E. coli* contamination issues. We therefore believe that a sampling campaign focused on wells used for drinking water would be necessary to enhance the reliability of contamination maps.

Temporal variability has not really been taken into account, as only one campaign made in the previous year can be compared to our results. The variation in concentration between 2016 and 2017 campaigns indicate that temporal variability should be investigated with water monitoring over 1 year, it would then include wet and dry season as seasonality could influence infiltration.

Ion concentration results show that saline intrusion is a major ion contributor, nevertheless, the influence of the saline intrusion decreases in the area of Tulum city center. This could be due to a thicker FWL linked to a lower hydraulic conductivity, but it needs to be investigated and confirmed with new piezometric measurements, especially in the area between Kaan Luum and the coast. If confirmed, this should be taken into account in case of pollution like, as example, a chemical leakage, as residence time and dilution could be modified compared to nearby areas.

Considering ions due to human inputs, phosphate concentrations that are often a threat for coral reefs remain low due to lack of agriculture and adsorption on calcite but in case of rising sea level, a heightened saline intrusion could increase desorption and thus phosphate input to the reef. Nitrates' high concentrations in the city center underline the need for an improvement in the wastewater facilities.

Acknowledgements The authors of this paper want to acknowledge the Swiss National Science Foundation for its financial support (contract 200021L_141298), the NGO Amigos De Sian Ka'an for its support in the field, Office Cantonal des Bourses d'Etude, Vincent Gruber for his technical advices when preparing the field campaign and the ion analysis, and Gregory Käser for his assistance when preparing the field work. Renaud Saint Loup acknowledges in addition the Fond des Donations of the University of Neuchâtel who funded his travel and field expenses in Tulum.

References

Bauer-Gottwein P, Gondwe BRN, Charvet G et al (2011) Review: the Yucatán peninsula karst aquifer, Mexico. Hydrogeol J 19:507–524. https://doi.org/10.1007/s10040-010-0699-5

Beddows PA (2004) Groundwater hydrology of a coastal conduit carbonate aquifer. Caribbean Coast of the Yucatan Peninsula, Mexico

Beddows PA, Smart PL, Whitaker FF, Smith SL (2007) Decoupled fresh–saline groundwater circulation of a coastal carbonate aquifer: spatial patterns of temperature and specific electrical conductivity. J Hydrol 346:18–32. https://doi.org/10.1016/j.jhydrol.2007.08.013

Dillon KS, Reide Corbett D, Chanton P et al (2000) Bimodal transport of a waste water plume injected into saline ground water of the Florida Keys. Groundwater 38(4):624–634

Gondwe BRN, Hong S-H, Wdowinski S, Bauer-Gottwein P (2010a) Hydrologic dynamics of the ground-water-dependent Sian Ka'an Wetlands, Mexico, derived from InSAR and SAR data. Wetlands 30:1–13. https://doi.org/10.1007/s13157-009-0016-z

Gondwe BRN, Lerer S, Stisen S et al (2010b) Hydrogeology of the south-eastern Yucatan Peninsula: New insights from water level measurements, geochemistry, geophysics and remote sensing. J Hydrol 389:1–17. https://doi.org/10.1016/j.jhydrol.2010.04.044

Gondwe BRN, Ottowitz D, Supper R et al (2012) Regional-scale airborne electromagnetic surveying of the Yucatan karst aquifer (Mexico): geological and hydrogeological interpretation. Hydrogeol J 20:1407–1425. https://doi.org/10.1007/s10040-012-0877-8

Hausman H (2009) Responsible Development in Tulum. Considering Water Quality and Subaqueous Cave Locations. Citeseer, Mexico

Hernández-Terrones L, Rebolledo-Vieyra M, Merino-Ibarra M et al (2011) Groundwater pollution in a karstic region (NE Yucatan): baseline nutrient content and flux to coastal ecosystems. Water Air Soil Pollut 218:517–528. https://doi.org/10.1007/s11270-010-0664-x

Leal-Bautista RM, Lenczewski M, Morgan C et al (2013) Assessing fecal contamination in groundwater from the Tulum Region, Quintana Roo, Mexico. J Environ Prot 04:1272–1279. https://doi.org/10.4236/jep.2013.411148

Lopez O (2016) Tulum, Mexico: how an eco-chic retreat became a den of corruption. Newsweek

Metcalfe CD, Beddows PA, Bouchot GG et al (2011) Contaminants in the coastal karst aquifer system along the Caribbean coast of the Yucatan Peninsula, Mexico. Environ Pollut 159:991–997. https://doi.org/10.1016/j.envpol.2010.11.031

Millero F, Huang F, Zhu X et al (2001) Adsorption and desorption of phosphate on calcite and aragonite in seawater. Aquat Geochem 7:33–56

Null KA, Knee KL, Crook ED et al (2014) Composition and fluxes of submarine groundwater along the Caribbean coast of the Yucatan Peninsula. Cont Shelf Res 77:38–50. https://doi.org/10.1016/j.csr.2014.01.011

Perry E, Paytan A, Pedersen B, Velazquez-Oliman G (2009) Groundwater geochemistry of the Yucatan Peninsula, Mexico: constraints on stratigraphy and hydrogeology. J Hydrol 367:27–40. https://doi.org/10.1016/j.jhydrol.2008.12.026

Rohling EJ, Fenton M, Jorissen FJ et al (1998) Magnitudes of sea-level lowstands of the past 500,000 years. Nature 394:162

Smart PL, Beddows PA, Coke J et al (2006) Cave development on the Caribbean coast of the Yucatan Peninsula, Quintana Roo, Mexico. In: Special Paper 404: Perspectives on Karst Geomorphology, Hydrology, and geochemistry—a tribute volume to Derek C. Ford and William B. White. Geological Society of America, pp 105–128

Turner BD, Binning P, Stipp SLS (2005) Fluoride removal by calcite: evidence for fluorite precipitation and surface adsorption. Environ Sci Technol 39:9561–9568. https://doi.org/10.1021/es0505090

Vengosh A, Pankratov I (1998) Chloride/bromide and chloride/fluoride ratios of domestic sewage effluents and associated contaminated ground water. Groundwater 36(5):815–824

Vuilleumier C, Borghi A, Renard P et al (2013) A method for the stochastic modeling of karstic systems accounting for geophysical data: an example of application in the region of Tulum, Yucatan Peninsula (Mexico). Hydrogeol J 21:529–544. https://doi.org/10.1007/s10040-012-0944-1

Ward WC (2003) Introduction to pleistocene geology of NE Quintana Roo. In: Salt Water Intrusion & Coastal Aquifer Conference (SWICA). Field Trip to the Caribbean Coast of the Yucatan Peninsula. pp 13–22

Ward WC, Keller G, Stinnesbeck W, Adatte T (1995) Yucatán subsurface stratigraphy: Implications and constraints for the Chicxulub impact. Geology 23:873. https://doi.org/10.1130/0091-7613(1995)023%3C0873:YNSSIA%3E2.3.CO;2

World Health Organisation (2003) Nitrate and nitrite in drinking water (background document for development of WHO Guidelines for Drinking water Quality). World Health rganisation. Report No. WHO/SDE/WSH/04.03/56, pp 16

Worthington SRH, Ford DC, Beddows PA (2000) Porosity and permeabilty enhancement in unconfined carbonate aquifers as a result of solution. In: Speleogenesis: evolution of karst aquifers. National Speleological society of America Huntsville, Alabama, pp 220–223